Evolutionary and Deterministic Methods for Design,
Optimization and Control with Applications to Industrial and Societal Problems
EUROGEN 2005
R. Schilling, W.Haase, J. Periaux, H. Baier, G. Bugeda (Eds)

SHAPE OPTIMIZATION OF FISH TAIL PROPULSION WITH HYDRO-ELASTIC EFFECTS

Eriko Shimizu[?], Shinkyu Jeong[*], Koji Isogai[†] and Shigeru Obayashi[‡]

[?] Integrated Fluid Informatics Laboratory,
Institute of Fluid Science,
Tohoku University, Japan
2-1-1 Katahira, Aoba-ku, Sendai, Japan
e-mail: shimizu@edge.ifs.tohoku.ac.jp, web page: http://www.ifs.tohoku.ac.jp/edge

[*] Integrated Fluid Informatics Laboratory,
Institute of Fluid Science,
Tohoku University, Japan
2-1-1 Katahira, Aoba-ku, Sendai, Japan
e-mail: jeong@edge.ifs.tohoku.ac.jp, web page: http://www.ifs.tohoku.ac.jp/edge

[†] Department of Aerospace Engineering,
Nihonbunri University, Japan
1727 Ooaza Ichigi, Ooita, Japan
e-mail: isogai@nbu.ac.jp

[‡] Integrated Fluid Informatics Laboratory,
Institute of Fluid Science,
Tohoku University, Japan
2-1-1 Katahira, Aoba-ku, Sendai, Japan
e-mail: obayashi@ifs.tohoku.ac.jp, web page: http://www.ifs.tohoku.ac.jp/edge

Key words: Oscillatory tail, Potential flow, Kriging model, Multidisciplinary Design

Abstract. Performance of a fish tail is brought out from many facters, such as shape, movement and material. The purpose of the present study is to reveal their relations by means of multidisciplinary design optimization. Kriging method and Adaptive Range Multi Objective Genetic Algorithms were used to reveal the structure of the design space. The relationship between the factors were revealed, and two specific types of the fish tails were obtained.

Nomenclature

Z	vertical displacement of the tail surface
X	chordwise position
Y	spanwise position
T	time
H_0	heaving amplitude
ω	frequency
X_p	axis of pitch
α_0	pitching amplitude
ϕ	phase advance angle of pitching oscillation ahead of heaving oscillation
Φ_i	i^{th} natural vibration mode
q_i	generalized coordinate
$\bar{C}_T$	thrust coefficient
$\bar{C}_{Tl}$	thrust coefficient due to the leading edge suction force
$\bar{C}_{Td}$	thrust coefficient due to the pressure which is perpendicular to the plane of the tail
η_p	propulsive efficiency
$\bar{T}$	time-avaraged thrust
V	flow velocity
$\bar{W}$	time-avarage power needed for tail oscillation
T^*	period of oscillation
S	tail area
P	pressure distribution on the wing

1 INTRODUCTION

In the long evolution process, marine creatures have developed various features suitable for refined swimming. Yellow fin tuna can swim at more than 70 km/h, while there are fishes with its radius of revolution of only 10 to 30% of body length. These preformances are remarkable compared to the present nautical engineering. Recently fish robots have been developed to obtain the high performances. Thanks to great efforts of researchers, now we can see fish robots, which can swim like fish. However, these robots have not been able to achieve high performances like fish, due to the fact that the machanism of fish swimming, especially the interaction between fluid and elastic deformation, is not well understood.

Considering the tail, tuna has a stiff lunate tail and gobioid has an elliptical elastic tail and their movements are also different. As a result the former has high propulsive efficiency and the later has high impulsive thrust. From these observations it is considered that thrust performance has a strong relationship with the tail shape, movement and elasticity.

Many studies have been conducted for shape or movement optimization of oscillatory

tail. However they performed the optimizations separately. Furthermore most of the researches do not consider the interaction between fluid and elastic deformation. Kuroda et al.[1] and Isogai et al.[2] have conducted movement optimization of a lunate tail to maximize the propulsive efficienty with hydro-elastic interaction [1]. Although the hydro-elastic interaction was considered, the objective function was only the propulsive efficiency and the design variables were only for the movement.

The aim of this study is reveal the mechanism of fish swiming by optimization. Based on the results of Kuroda et al. and Isogai et al., this research considers multi-objective optimization with other factors for design variables. Multi-objective optimization reveals the structure of the design space from the trade-off information, and design variables considering with not only the shape, but also the movement and the elasticity reveal the interactions and the relationships with swiming performances. Response surface and Adaptive Range Multi-Objective Genetic Algorithms (ARMOGA) have been coupled and used to obtain design space information.

2 APPROACH

2.1 Model and objective functions

In the analysis model, the tail shape is simplified and defined by aspect ratio, taper ratio and sweep angle. The movement consists of heaving and pitching oscillations, and the pitching oscillation has the phase advance angle ϕ ahead of the heaving oscillation. Considering the tail elasticity, the displacement of the tail is defined as follows.

$$Z(X,Y,T) = H_0 sin(\omega T) - (X - X_p)\alpha_0 sin(\omega T + \phi) + \sum \Phi_i(X,Y) q_i(T) \qquad (1)$$

where Z is the vertical displacement of the tail surface, and on the right-hand side, the first term is a contribution by the forced heaving oscillation, the second term is one by the forced pitching oscillation and the third term is the one by the elastic deformation.

Thrust coefficient and propulsive efficiency are used to evaluate tail performances. These are defined as follows.

$$\bar{C}_T = \bar{C}_{Tl} + \bar{C}_{Td} \qquad (2)$$

$$\eta_p = \frac{\bar{T}V}{\bar{W}} \qquad (3)$$

where,

$$\bar{W} = \frac{1}{T^*} \int_0^{T^*} \left(\int_S \Delta P(X,Y,Z) \frac{dZ}{dT} dX dY \right) dT$$

In the present study the root semi chord length is 0.05[m], the thickness of the tail is 0.001 [m]. Flow velocity is 2 [m/s]. Kinematical viscosity of water is about 1.00×10^{-6}. Thus the Reynolds number based on root semichord is 10^5.

2.2 Evaluation

To obtain the thrust coefficient and the propulsive efficiency, Modified Doublet Lattice Method (MDLM) and Finit Element Method (FEM) are used. MDLM is used for the flow calculation. FEM is used for strucured analysis.

MDLM is an extension of Doublet Lattice Method (DLM)[3], which is suitable for the calculation of the unsteady fluid force for an arbitrary shape of a wing. While DLM does not consider the leading-edge suction, MDLM is improved to calculate the leading-edge suction force at the same time. The leading-edge suction force[4] is the suction due to the flow around the leading-edge of a thin wing.

The potential flow theory is chosen for the present optimization because it is computationally inexpensive. DLM is based on the potential theory, it does not consider viscosity. When a fish needs thrust, dynamic stall vortex, which prevents the tail from increasing propulsive efficiency, is not desirable. Thus it is considered that basically a fish does not have the dynamic stall vortex on the tail while crusing. Constraint is given to keep the flow analysis valid by avoiding the dynamic stall, that is, by limiting the effective angle of attack to less than 8 degrees.

2.3 Optimization

In this study objective functions are the thrust coefficient and the propulsive efficiency (equations 2 and 3). Design variables and their ranges are shown in table 1. Heaving amplitude and axis of pitch are normalized by the root semi-chord length. A negative value of the axis of pitch indicates the leading-edge side, a plus value of the axis of pitch indicates the trailing-edge side.

First of all, sample points are generated using Latin Hypercube Sampling (LHS)[5], one of Design Of Experiment(DOE) methods. In this method, the range of the input variable is divided into N strata equally, and sample one from each stratum. Thus, it is ensured that each of the input variable has all portions of its distribution. Even when the output is dominated by only a few of the input components, this method ensures that each of those components is represented in a fully strarified manner, no matter which components might turn out to be important. Here, it is also made sure that the generated solutions satisfy the constraint.

Next, response surface is generated from the solutions using the Kriging model[6]. In the present study the Kriging model is formed using the solutions at the sample points generated by LHS to obtain equal accuracy for the whole design space.

Optimization to maximize the thrust coefficient and the propulsive efficiency is done on the response surface using ARMOGA[7]. This method searchs a large design space efficiently by the range adaptation.

	Design variable	lower value (bound)	upper value (bound)
Shape	Aspect ratio	1	10
	Taper ratio	0.1	1.0
	Sweep angle [deg]	0.0	50.0
Movement	Heaving amplitude	0.5	3.0
	Pitching amplitude [deg]	0.0	30.0
	Reduced frequency	0.03	0.5
	Axis of pitch	-1.0	1.0
	Phase advance angle of pitching oscillation ahead of heaving oscillation [deg]	10	140
Elasticity	Young's modulus [Pa]	10^3	10^{11}
	Poisson ratio	0.3	0.5
	Density [kg/m^3]	800	70000

Table 1: Ranges of design variables

3 RESULTS AND DISCUSSIONS

In figure 1, all solutions obtained from ARMOGA were plotted by the two objective functions, and non-dominated solutions were shown by red squares. These non-dominated solutions show trade-off between the thrust coefficient and the propulsive efficiency, the non-dominated front seems to consist of two curves.

To analyze the solutions in detail, the computed thrust coefficients were plotted by the design variables. From these results, it was found that the solutions can be divided into two groups by the aspect ratio (in figure 2). Figure 2 shows the thrust coefficient versus aspect ratio. We can see two peaks in the profile of the thrust coefficient. When the aspect ratio is around 2, the solutions tend to have high values in the thrust coefficient and low values in the propulsive efficiency. On the other hand, when the aspect ratio is around 9, the solutions tend to have low values in the thrust coefficient and high values in the propulsive efficiency.

Because the aspect ratio has a strong effect on the thrust coefficient, all plots in figure 1 were colored by aspect ratio as shown in figure 3. Non-dominated solutions are shown as squares. In this figure two groups are recognized. One is the group that has a low aspect ratio and the other is the group that has a high aspect ratio. Two non-dominated fronts are formed by these two groups. The former group will be called Group A, latter group will be called Group B.

Figures 3 to 11 show all solutions plotted by the two objective functions and colored according to the respective design variables. From these figures, ranges of non-dominated solutions are given in table 2. Figures 6 and 7 indicate that the tail oscillation of Group

A is larger than that of Group B.
When the thrust coefficient is high, as seen in figure 8, the reduced frequency tends to be large up to 0.40. On the other hand, when propulsive efficiency is high, the reduced frequency becomes small. Therefore, Group A oscillates faster than Group B. Frequency of Group A corresponds to 2.2[Hz], while that of Group B corresponds to 1.5[Hz].

In figure 10, Group B has the phase advance angle around 90[deg]. Many past studies found that this phase advance angle is ideal for fish swiming. Group A takes this value at 75[deg]. Isogai et al.[2] suggested that 75[deg] is the ideal phase advance angle for dolphin swimming, with high propulsive efficiency.
From figure 11, it is clear that improving thrust coefficient requires stiffness, but improving propulsive efficiency requires some flexibility. In figure 12, solutions in Group A has poisson ratios above 0.4, while Group B has those below 0.4. From figure 13 no trend is found about density. It may be difficult to specify poisson ratio and young's modulus arbitrarily, because existing materials may not have the required properties. It is also difficult to find which natural viblation modes are important factors for thrust performances from these results.

Table 3 shows typical solutions for Group A and Group B. The thrust coefficient and propulsive efficiency were recalculated using MDLM and FEM. Characteristics of Group A is as follows. Group A has a higher thrust coefficient but a lower propulsive efficiency than Group B. The shape has a low aspect ratio, a high taper ratio and a low sweep angle (figure 14). The movement is a large flapping motion with a high frequency. The material needs stiffness. Characteristics of Group B is as follows. GroupB has a lower thrust coefficient but a higher propulsive efficiency than Group A. The shape has a high aspect ratio, a low taper ratio and a high sweep angle (figure 15). The movement is a small flapping motion with relatively low frequency. The material needs some flexibility. These characteristics are simillar to those of natural fish. The fish tail that has a high propulsive efficiency has a high aspect ratio and its movement is not so large and not so fast, such as a tuna. On the other hand, the fish that has a high thrust coefficient has a low aspect ratio, and its movement is large and fast, such as a gobioid.

4 CONCLUSIONS

This study has revealed the relationship between the shape, the movement and the elasticity of the fish tail by means of multi objective design optimization.

The Kriging model and ARMOGA have been applied to design the oscillatory tail by maximizing the thrust coefficient and propulsive efficiency. The Kriging model was used to make the response surface and ARMOGA was used to reveal the trade-off information of design space from the response surface. The results have indicated that oscillatory tails can be divided into two groups by the aspect ratio. One group is superior in the thrust

Design variable	Group A	Group B
Thrust coefficient	High	Low
Propulsive efficiency	Low	High
Aspect ratio	[1.50, 2.50]	[9.00, 9.50]
Tapre ratio	[0.74, 0.85]	[0.87, 0.97]
Sweep angle [deg]	[0.00, 15.0]	[24.0, 33.0]
Heaving amplitude	[2.25, 2.85]	[1.95, 2.50]
Pitching amplitude [deg]	[25.0, 29.0]	[19.0, 25.5]
Reduced frequency	[0.30, 0.35]	[0.22, 0.25]
Axis of pitch	[-0.4, 0.00]	[0.45, 0.70]
Phase advance angle [deg]	[86.0, 98.0]	[69.0, 72.0]
Young's modulus [Pa]	[8.40, 10.8]	[9.30, 10.0]
Poisson ratio	[0.40, 0.45]	[0.33, 0.40]
Density [kg/m^3]	[3000, 6500]	[3800, 6200]

Table 2: Ranges of design variables of non-dominated solutions.

coefficient, but not in the propulsive efficiency. The corresponding shape has a low aspect ratio, a high taper ratio, and a low sweep angle. The movement is a large flapping motion with a high frequency. The material needs stiffness. The other group is superior in the propulsive efficiency, but not in the thrust coefficient. The shape has a high aspect ratio, a high taper ratio, and a high sweep angle. The movement is a small flapping motion with a low frequency. The material needs flexibility. These characteristics are simillar to natural fish.

REFERENCES

[1] M. Kuroda, T. Ukimura, K. Isogai, Propulsive performance of lunate wing with aeroelastic effect, 34th Conference of Fluid Dynamics, 261-264, 2002.

[2] K. Isogai, D. Kariyazaki, M. Matsubara, and H. Yamazaki, Propulsive performance of dolphin's tail-fin -Optimum design of fin motion and its experimental validation-,36th Conference of Fluid Dynamics, 293-296, 2004.

[3] E. Albuno, and W. P. Rodden, A Doublet-Lattice Method for Clculating Lift Distributions on Oscillating Surfaces in Subsonic Flow, AIAA Journal, Vol. 7, No. 2, 279-285, 1969.

[4] C. E. Lan, The Unsteady Quasi-Vortex-Lattice Method with Applications to Animal Propulsion, Journal of Fluid Mechanics, Vol. 93, Part4, 747-765, 1979.

[5] M. D. McKay, R. J. beckman, and W. J. Conover, A Comparison of Three Methods for Selecting Values of Input Variables in the Analysis of Output from a Computer Code, Journal of Technometrics, Vol. 21, No. 2, 239-245, 1979.

[6] S. Jeong, M. Murayama, K. Yamamoto, Efficient Optimization Design Method Using Kriging Model, Journal of Aircraft, Vol. 42, 2005, 413-420.

[7] D. Sasaki, and S. Obayashi, Efficient Search for Trade-Offs by Adaptive Range Multi-objective Genetic Algorithms, Journal of Aerospace Computing Information, and Communication, Vol. 2, No.1, 44-64, 2005.

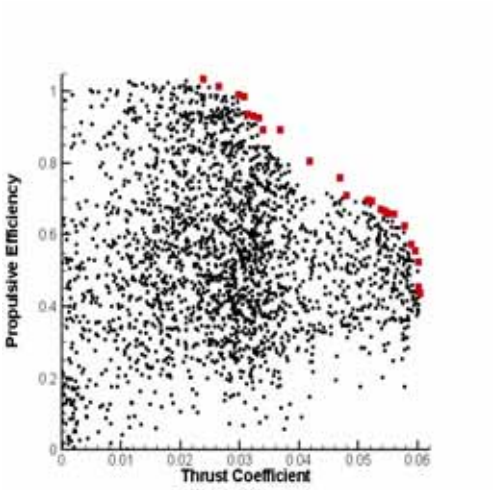

Figure 1: Solutions plotted by the object functions and non-dominated solutions are colored in red

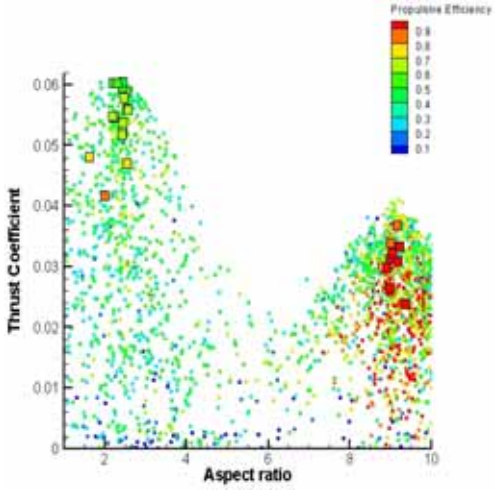

Figure 2: Solutions plotted by thrust coefficient and aspect ratio. Solutions are colored by propulsive efficiency

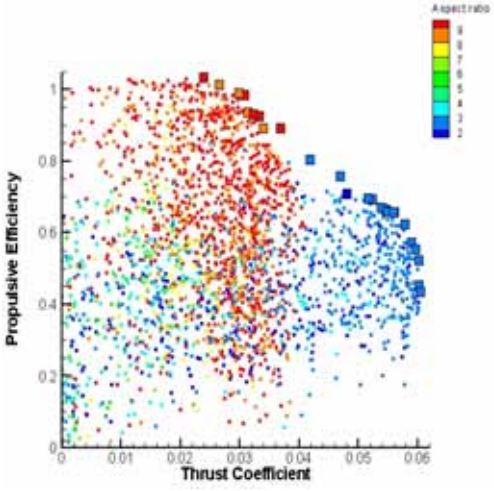

Figure 3: Solutions plotted by the object functions and colord by the aspect ratio

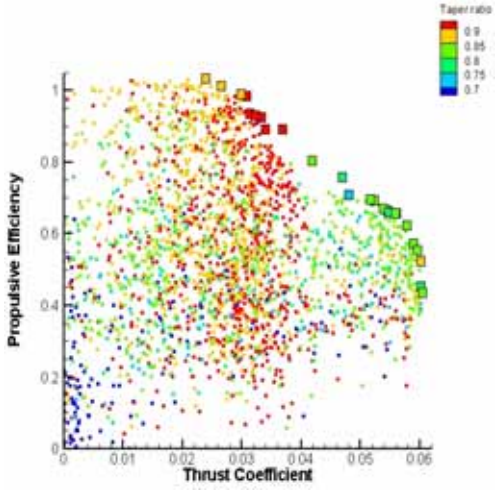

Figure 4: Solutions plotted by the object functions and colord by the taper ratio

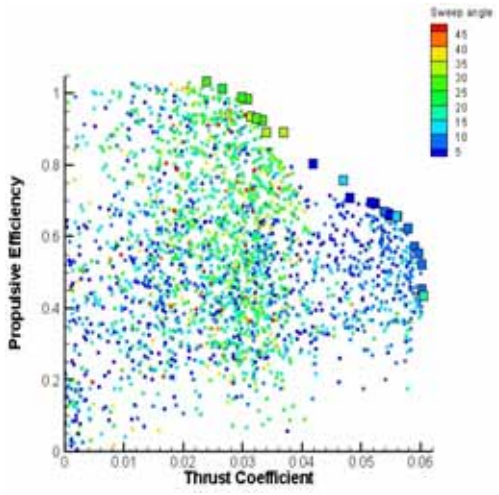

Figure 5: Solutions plotted by the object functions and colored by the sweep angle

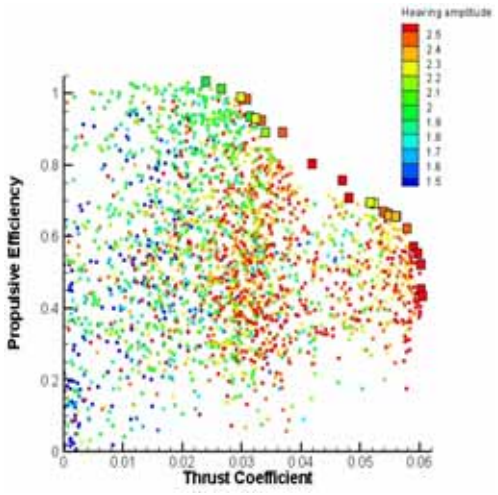

Figure 6: Solutions plotted by the object functions and colored by the heaving amplitude

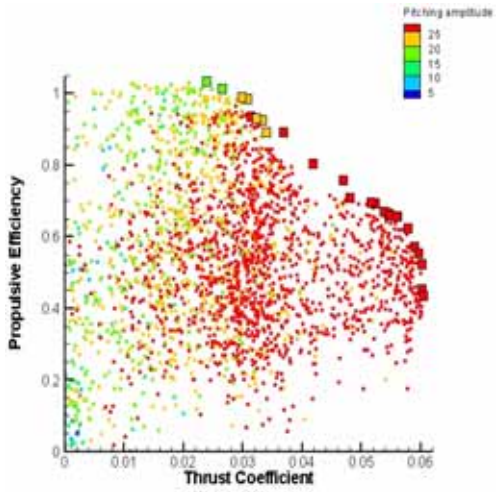

Figure 7: Solutions plotted by the object functions and colored by the pitching amplitude

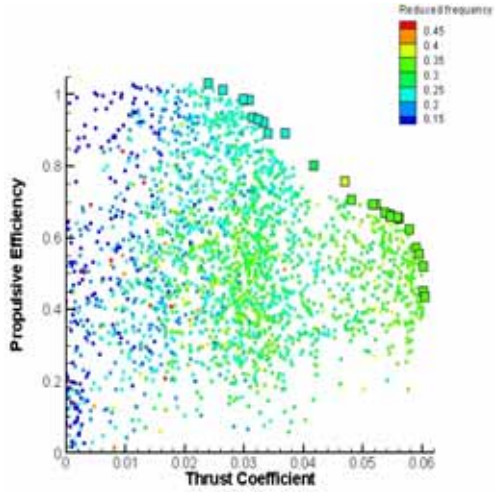

Figure 8: Solutions plotted by the object functions and colored by the reduced frequency

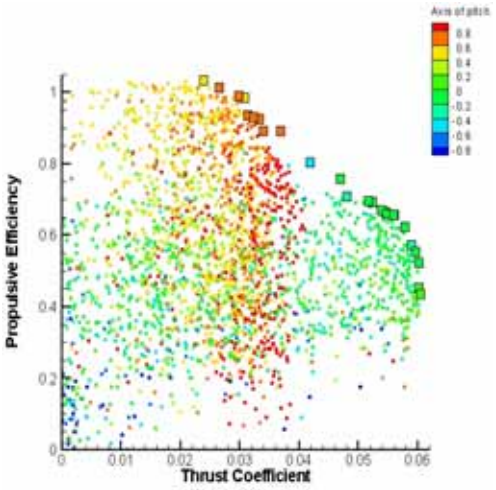

Figure 9: Solutions plotted by the object functions and colored by the axis of pitch

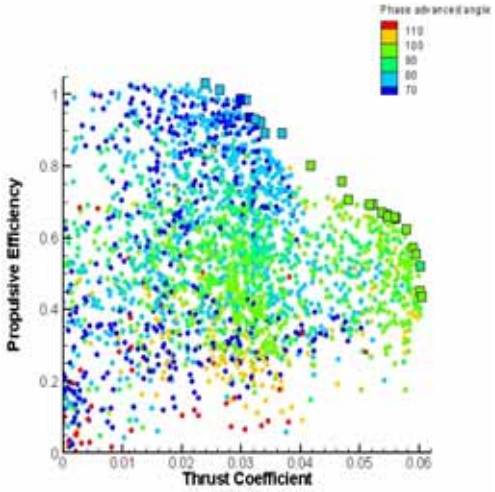

Figure 10: Solutions plotted by the object functions and colored by the phase advance angle of pitching oscillation ahead of the heaving oscillation

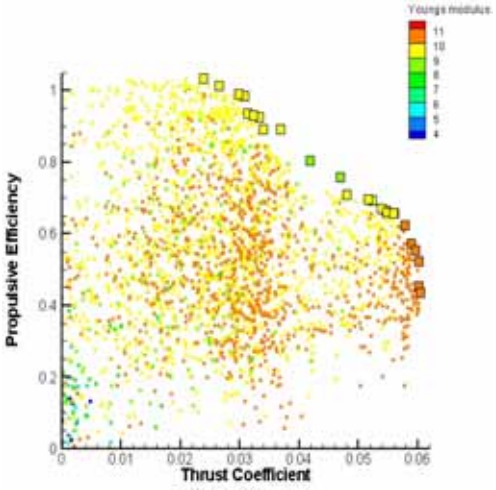

Figure 11: Solutions plotted by the object functions and colored by the young's modulus

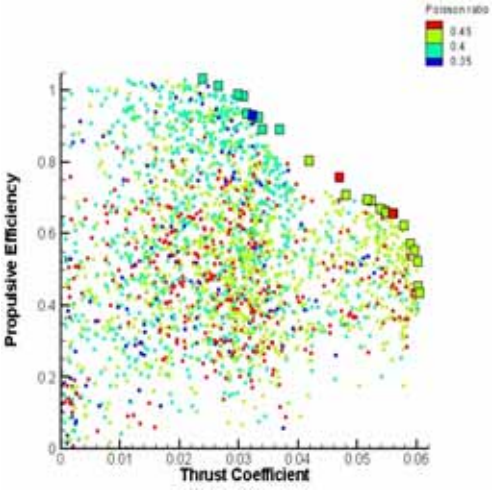

Figure 12: Solutions plotted by the object functions and colored by the poisson ratio

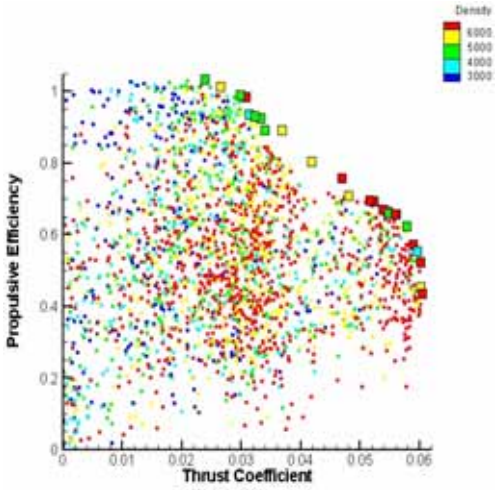

Figure 13: Solutions plotted by the object functions and colored by the density

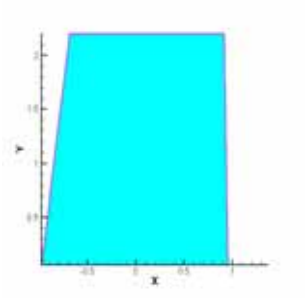

Figure 14: Typical shape of a tail which from Group A

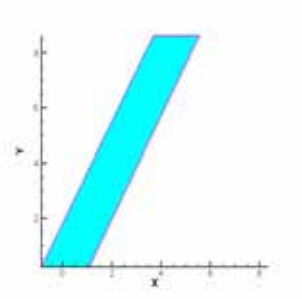

Figure 15: Typical shape of a tail from Group B

Design variable	Group A	Group B
Thrust coefficient	0.0917	0.0344
Propulsive efficienty	0.529	0.957
Aspect ratio	2.426	8.992
Tapre ratio	0.819	0.969
Sweep angle [deg]	5.362	31.67
Heaving amplitude	2.603	2.118
Pitching amplitude [deg]	25.70	24.68
Reduced frequency	0.312	0.234
Axis of pitch	-0.081	0.664
Phase advance angle [deg]	90.87	72.26
Young's modulus [Pa]	10.71	9.615
Poisson ratio	0.447	0.359
Density [kg/m^3]	3036	4099

Table 3: typical solutions from Group A and Group B